

Original Article

Fluorescence bioimaging analysis of collagen antibody-induced arthritis in male mice

Jin Seok Kang*

Department of Biomedical Laboratory Science, Namseoul University, Cheonan 31020, Korea

The purpose of this study was to investigate the lesions of a mouse collagen antibody-induced arthritis (CAIA) model using fluorescence bioimaging and micro-computed tomography (micro-CT) and to compare it with histopathological examination. Twelve mice were randomly divided into three groups: group 1 (G1) as control, group 2 (G2) as fluorescence probe control and group 3 (G3) as collagen antibody-induced arthritis. The mice of G3 intravenously received anti-type II collagen 5-clone antibody cocktail (2 mg/mouse) on day 0 and intraperitoneally received lipopolysaccharide (50 µg/mouse) on day 3. On the while, the mice of G1 and G2 received 0.9% saline in equal volumes at equivalent times. Fluorescence bioimaging and micro-CT analysis were carried out to assess arthritis. Treatment with the collagen antibody cocktail increased the paw thickness of mice compared to those in both the control and probe-treated groups. Fluorescence bioimaging using a near infrared imaging agent showed high intensity in the joints of collagen antibody-treated mice, whereas those of control mice showed no signal. Micro-CT analysis of the knee joints of collagen antibody-treated mice showed rough and irregular articular appearance, whereas those of control mice showed normal appearance. Histopathological examination of the knee joints of collagen antibody-treated mice revealed destruction of cartilage and bony structure, synovial hyperplasia and infiltration of inflammatory cells. No cartilage destruction or inflammation was observed in control or probe control mice. Taken together, it is concluded that analyses of fluorescent bioimaging made it possible to evaluate CAIA lesions, comparable with those by micro-CT and histopathological examination in mice.

Key words: mice, arthritis, fluorescence bioimaging, micro-computed tomography, histopathology

Introduction

Rheumatoid arthritis (RA) represents cartilage and bone destruction, persistent synovitis and systemic inflammation [1]. Among several mouse RA models, the collagen antibody-induced arthritis (CAIA) model shows good similarity with human RA and is usually used to investigate pathogenic mechanisms of RA [2, 3]. A cocktail of collagen type II-specific monoclonal antibodies has been used to induce an acute form of arthritis in experimental animals [4]. Modification of the cocktail to enhance its arthritogenicity has induced severe and consistent arthritis, even in low responder strains [5].

For *in vivo* monitoring of arthritis progression, it is necessary to visualize the real presentation of pathological lesions in experimental animals. Modern several imaging technologies enable the detection and visualization of biological processes [6], and provide the data related to several disease progression [7, 8] and 3D structures of tissues [9], and reduce the number of animals required for experiments [10]. Also, they even supply quantitative results [11]. High-resolution micro-computed tomography (micro-CT) has advantage over other modalities for the imaging of bony structures and is primarily used to detect bony changes in experimental animals [12]. However, it is limited in its ability to detect slight or minimal alterations in joints, especially in cartilage [13]. To overcome this, optical imaging using fluorescence probes has been used for the detection of altered biomolecules [14]. Near-infrared fluorescence imaging agents have been utilized to detect several pathological changes such as apoptosis [15] and oxidative stress [16].

Even though near-infrared spectroscopic probing could be used to detect changes in the composition of the subchondral bone and might distinguish healthy cases from osteoarthritis in rats [17], there have been a few reports about *in vivo* monitoring of mouse RA using near-infra-

*Corresponding author: Jin Seok Kang

red probes. The purpose of this study was to examine CAIA lesions using fluorescence imaging and to compare the results with those of micro-CT and histopathological examination.

Materials and Methods

Introduction of arthritis

Male BALB/c mice were obtained from Nara Biotech Co. Ltd. (Seoul, Korea) at 6 weeks old of age. The mice were kept in a room with $22 \pm 3^\circ\text{C}$, $55 \pm 5\%$ and a 12-h light/dark cycle. Mice were fed filtered water ad libitum and unrefined chlorophyll-containing ingredients in an alfalfa free diet (Harlan Laboratories, Inc., Madison, WI). After one week for acclimation, twelve mice were randomly divided into three groups: group 1 (G1) as control animals, group 2 (G2) as fluorescence probe control animals and group 3 (G3) as animals with collagen antibody-induced arthritis. The mice of G3 intravenously received anti-type II collagen 5-clone antibody cocktail (Chondrex, Redmond, WA) (2 mg/mouse) on day 0 and intraperitoneally received lipopolysaccharide (LPS, Chondrex) (50 $\mu\text{g}/\text{mouse}$) on day 3. On the while, the mice of G1 and G2 received 0.9% saline in equal volumes at equivalent times.

Fluorescence bioimaging

Veet cream was used for removal of hair before the process of fluorescence bioimaging. Mice in G1 received equal volumes of 0.9% saline. Mice in G2 and G3 were injected intravenously with OsteoSense[®] 680 EX (PerkinElmer, Waltham, MA) at the dose of 2 nmol/100 μl /mouse on day 7 post collagen cocktail treatment. Fluorescence bioimaging was taken by IVIS Lumina Series III (PerkinElmer) at 48 h after near-infrared probe treatment under anesthesia with avertin (Sigma, Saint Louis, MO).

All mice were sacrificed at day 9, and the knee joints

were fixed in 10% neutral phosphate-buffered formalin. This study was approved by the animal experiment committee of Namseoul University based on the Animal Protection Act.

Micro-CT analysis

A micro-CT system (Skyscan1173, Bruker, Kontich, Belgium) was used for analysis of the knee joints. The specimens were scanned with an X-ray source of 75 kV/106 μV and pixel size of 9.94 μm using an aluminum 1.0-mm filter. After scanning, cross-sectional slices were reconstructed by NRecon software Ver.1.6.9.16 (Bruker). Three-dimensional analysis was performed using CT Analyser Ver. 1.14.4.1 (Bruker).

Histopathological observation

Fixed samples were decalcified in 14% EDTA-glycerol for 14 days at room temperature and were routinely processed and embedded in paraffin. Slide sections were stained with hematoxylin and eosin (H&E) for histopathological examination.

Statistical analysis

Statistical analyses were performed using GraphPad Prism 6 (GraphPad Software, La Jolla, CA). All data were analyzed using Dunnett's multiple comparison test following one-way analysis of variance and Student's t-test. P-values of <0.05 were considered statistically significant.

Results

Introduction of arthritis

Measurable macroscopic changes were determined by paw thickness measurement. Normal paw appearance was shown in G1 and G2. However, the paw thickness of G3 was increased on day 6 after the treatment with anti-type II collagen 5-clone antibody cocktail (Fig. 1).

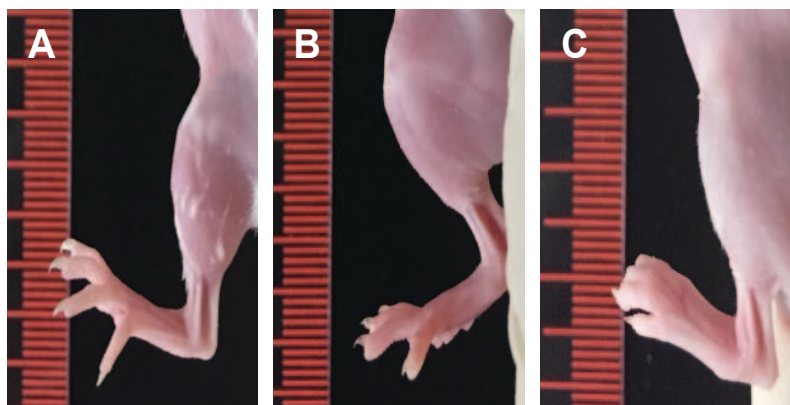


Fig. 1. Macroscopic views of the joints in mice. (A) A control mouse (G1), (B) A fluorescence probe control mouse (G2), and (C) An arthritis-induced mouse (G3) at day 6 after treatment of anti-type II collagen 5-clone antibody cocktail. Note the normal appearances of the joints in G1 and G2. However, the paw thickness was dramatically increased in G3 treated with anti-type II collagen 5-clone antibody cocktail.

Fluorescence bioimaging

Analysis of fluorescence bioimaging showed that no fluorescence was observed in G1. Fluorescence intensity was observed in G2 and G3, with G3 showing greater intensity than G2 at 24 h after OsteoSense[®] 680 EX treatment (Fig. 2).

Micro-CT analysis

Micro-CT analyses showed that joint surfaces in G1 and G2 represented normal articular appearance. However, in G3, micro-CT images showed irregular articular appearance (Fig. 3). It showed a diffuse pattern mainly located on the articular surface.

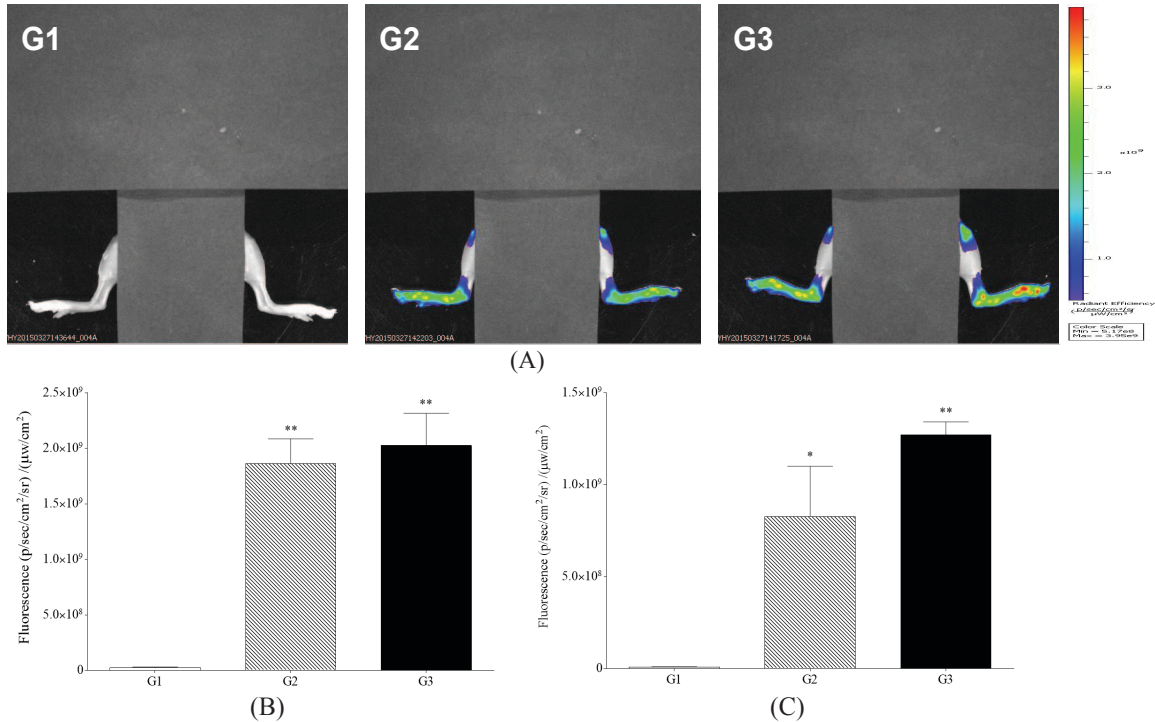


Fig. 2. Detection of fluorescence bioimaging by Lumina III. (A) G1 as a control mouse, G2 as a probe control mouse, G3 as an arthritis-induced mouse, (B) Fluorescence intensity in the ankle joints of mice, and (C) Fluorescence intensity in the knee joints of mice. *,** Significant different from G1 ($p < 0.05$, $p < 0.01$, respectively).

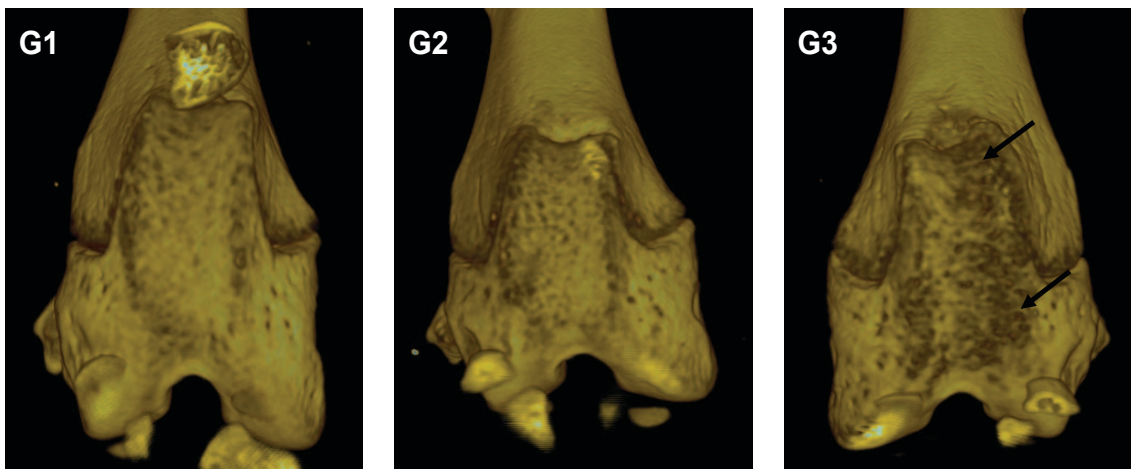


Fig. 3. Three-dimensional visualization of bony structures in the hind knee joint of CAIA mouse by micro-CT. (A) G1 as a control mouse, (B) G2 as a probe control mouse, and (C) G3 as an arthritis-induced mouse. Note the joint surfaces of G1 or G2 as normal articular appearance. However, G3 showed irregular articular appearance (arrows).

Histopathological observation

No cartilage destruction or inflammation was found in G1 and G2. However, G3 showed destruction of the cartilage with degeneration of chondrocytes. Furthermore, the destruction of articular surfaces of joints in G3 showed destruction of bony structures, as well as synovial hyperplasia and infiltration of inflammatory cells, mainly consisted of neutrophils (Fig. 4).

Discussion

In this study, fluorescence bioimaging and micro-CT provided information for the assessment of arthritis lesions, and these results generally agreed with histopathology assessment.

When examining arthritis lesions *in vivo*, bioimaging enables detection of several molecules and visualization of biological processes [6]. In this study, OsteoSense® 680EX as fluorescence bioimaging probe was tested *in vivo*. A near-infrared bioimaging agent, OsteoSense® 680EX, is basically designed to emit the light by binding to hydroxyapatite for the detection of microcalcification areas and bone remodeling lesions. Compared to G1, fluorescence intensity in G2 and G3, with G3 showing higher intensity than G2. Furthermore, this fluorescence-based imaging has some limitations in its ability to detect the anatomical location of lesions. Although bioimaging using near-infrared probe(s) may provide tissue detection and potential quantification [18], in this study, a high background level of fluorescence signals was observed in G2, even though G3 showed higher intensity compared to G2. Further studies will be warranted to develop the specific fluorescence probe(s) capable of detecting the disease progression of arthritis, with low background level.

This study used micro-CT to analyze alterations in bone structures. Micro-CT analyses showed that joint surfaces

in G3 showed degeneration of articular surface and alteration of bony structures. This was consistent with disruption of synovial membrane and structural changes in bony tissues revealed by HE examination. Although micro-CT analysis identified damaged areas in the articular surface, it may have the possibility not to detect the pathological lesions, especially when the lesions are restricted to small areas. And as there may be some limitations to current methods for quantification of pathological lesions, the development of new techniques is necessary [19]. Three-dimensional visualization of lesions may be one of these new approaches [20]. Further studies into the examination of arthritis lesions via different bioimaging techniques, especially 3D approaches, are warranted.

Among several RA animal models, the CAIA is an acute arthritis model that induces rapid onset of disease, usually with an experimental period of two weeks [2]. In this study, arthritis lesions occurred from day 5 to 9 after collagen antibody injection. However, the CIA model induces gradual onset of disease, usually with an experimental period of four weeks, showing hypertrophy of the synovial lining in early inflammatory arthritis and formation of fibrovascular pannus in the later stage of the disease [21]. For the rapid screening, the acute RA model is preferred. However, animal variation should be considered and the proper RA model should be selected according to research purpose and target molecules.

Taken together, analyses of fluorescence bioimaging using OsteoSense® 680EX probe made it possible to evaluate CAIA lesions, comparable with micro-CT and histopathological examination in mice. However, it had some limitations when used with fluorescence owing to a high background level of fluorescence signals.

Acknowledgements

I would like to thank Ms. Joo Hye Sim for her techni-

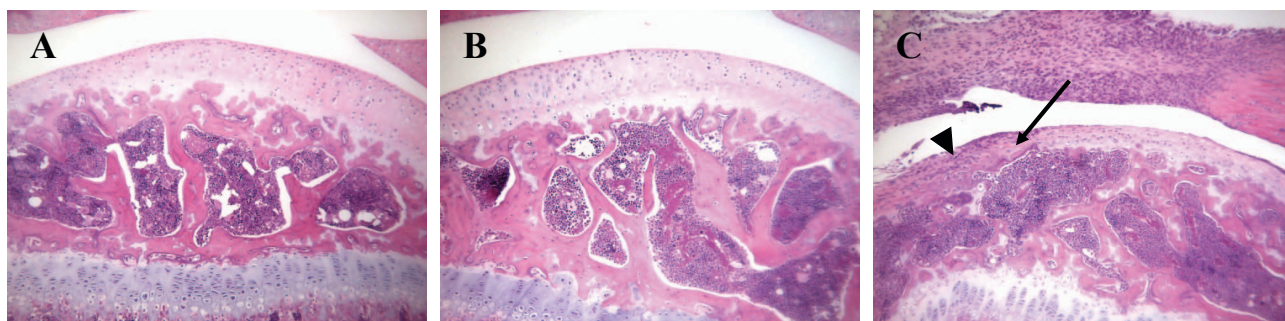


Fig. 4. Histopathological examination of the knee joints in mice. (A) G1 as a control mouse, (B) G2 as a probe control mouse, and (C) G3 as an arthritis-induced mouse. Note the normal appearance of the joint in a control mouse (A) and a probe control mouse (B). However, joint destruction is remarkable in G3, showing degeneration and destruction of cartilage and bone (arrow) and infiltration of inflammatory cells (arrow head). H&E staining, x100.

cal assistance. Funding for this paper was provided by Namseoul University.

ORCID

Jin Seok Kang, <http://orcid.org/0000-0002-4492-3101>

Reference

1. Scott DL, Wolfe F, Huizinga TW. Rheumatoid arthritis. *Lancet* 2010;376:1094-1108.
2. Khachigian LM. Collagen antibody-induced arthritis. *Nature protocols* 2006;1:2512-6.
3. Oestergaard S, Rasmussen KE, Doyle N, et al. Evaluation of cartilage and bone degradation in a murine collagen antibody-induced arthritis model. *Scandinavian journal of immunology* 2008;67:304-12.
4. Nandakumar KS, Svensson L, Holmdahl R. Collagen type II-specific monoclonal antibody-induced arthritis in mice: description of the disease and the influence of age, sex, and genes. *Am J Pathol* 2003;163:1827-1837.
5. Hutamekalin P, Saito T, Yamaki K, et al. Collagen antibody-induced arthritis in mice: development of a new arthritogenic 5-clone cocktail of monoclonal anti-type II collagen antibodies. *Journal of immunological methods* 2009;343:49-55.
6. Ying X, Monticello TM. Modern imaging technologies in toxicologic pathology: An overview. *Toxicol Pathol* 2006;34:815-826.
7. Chen Y, Liang CP, Liu Y, et al. Review of advanced imaging techniques. *Journal of pathology informatics* 2012;3:22.
8. Huh YM, Jun YW, Song HT, et al. In vivo magnetic resonance detection of cancer by using multifunctional magnetic nanocrystals. *J Am Chem Soc* 2005;127:12387-12391.
9. Tempel-Brami C, Schiffenbauer YS, Nyska A, et al. Practical Applications of in Vivo and ex Vivo MRI in Toxicologic Pathology Using a Novel High-performance Compact MRI System. *Toxicol Pathol* 2015;43:633-650.
10. de Jong M, Essers J, van Weerden WM. Imaging pre-clinical tumour models: improving translational power. *Nat Rev Cancer* 2014;14:481-493.
11. Provencher SW. Automatic quantitation of localized in vivo 1H spectra with LCModel. *NMR in biomedicine* 2001;14:260-264.
12. Schambach SJ, Bag S, Schilling L, et al. Application of micro-CT in small animal imaging. *Methods* 2010;50:2-13.
13. Kim YH, Kang JS. Effect of methotrexate on collagen-induced arthritis assessed by micro-computed tomography and histopathological examination in female rats. *Biomolecules & therapeutics* 2015;23:195-200.
14. Weissleder R, Tung CH, Mahmood U, et al. In vivo imaging of tumors with protease-activated near-infrared fluorescent probes. *Nat Biotechnol* 1999;17:375-378.
15. Jung HK, Wang K, Jung MK, et al. In vivo near-infrared fluorescence imaging of apoptosis using histone H1-targeting peptide probe after anti-cancer treatment with cisplatin and cetuximab for early decision on tumor response. *PloS one* 2014;9:e100341.
16. Shuhendler AJ, Pu K, Cui L, et al. Real-time imaging of oxidative and nitrosative stress in the liver of live animals for drug-toxicity testing. *Nat Biotechnol* 2014;32:373-380.
17. Afara IO, Prasadam I, Crawford R, et al. Near infrared (NIR) absorption spectra correlates with subchondral bone micro-CT parameters in osteoarthritic rat models. *Bone* 2013;53:350-357.
18. Peterson JD, Labranche TP, Vasquez KO, et al. Optical tomographic imaging discriminates between disease-modifying anti-rheumatic drug (DMARD) and non-DMARD efficacy in collagen antibody-induced arthritis. *Arthritis research & therapy* 2010;12:R105.
19. Cernohorsky P, Kok AC, Bruin DM, et al. Comparison of optical coherence tomography and histopathology in quantitative assessment of goat talus articular cartilage. *Acta orthopaedica* 2015;86:257-263.
20. Jain M, Robinson BD, Salamon B, et al. Rapid evaluation of fresh ex vivo kidney tissue with full-field optical coherence tomography. *Journal of pathology informatics* 2015;6:53.
21. Knoerzer DB, Donovan MG, Schwartz BD, et al. Clinical and histological assessment of collagen-induced arthritis progression in the diabetes-resistant BB/Wor rat. *Toxicol Pathol* 1997;25:13-19.